

Supplementary Information to accompany

Valence tautomerism and spin crossover in pyridinophane-cobalt-dioxolene complexes: an experimental and computational study†

Tina Tezgerevska,^a Elodie Rousset,^a Robert W. Gable,^a Guy N. L. Jameson,^a E. Carolina Sañudo,^b Alyona Starikova^c and Colette Boskovic*^a

Table S1 Continuous symmetry parameters (Shape) calculated for 6-coordinate metal complexes in compounds **1a**·dioxane, **2a**·2dioxane, **3a**·1.5dioxane and **4a**·2MeOH.¹

Shape Indices ^a	1a ·dioxane	2a ·2dioxane	3a ·1.5dioxane	4a ·2MeOH
<i>HP-6</i>	32.115	33.106	31.333	28.777
<i>PPY-6</i>	24.120	24.914	22.776	19.495
<i>OC-6</i>	1.378	0.935	3.102	3.974
<i>TPR-6</i>	10.160	11.894	9.436	7.373
<i>JPPY-6</i>	28.023	29.226	25.190	21.980

^a *HP*: Hexagon; *PPY*: Pentagonal pyramid; *OC*: Octahedron; *TPR*: Trigonal Prism; *JPPY*: Johnson pentagonal pyramid.

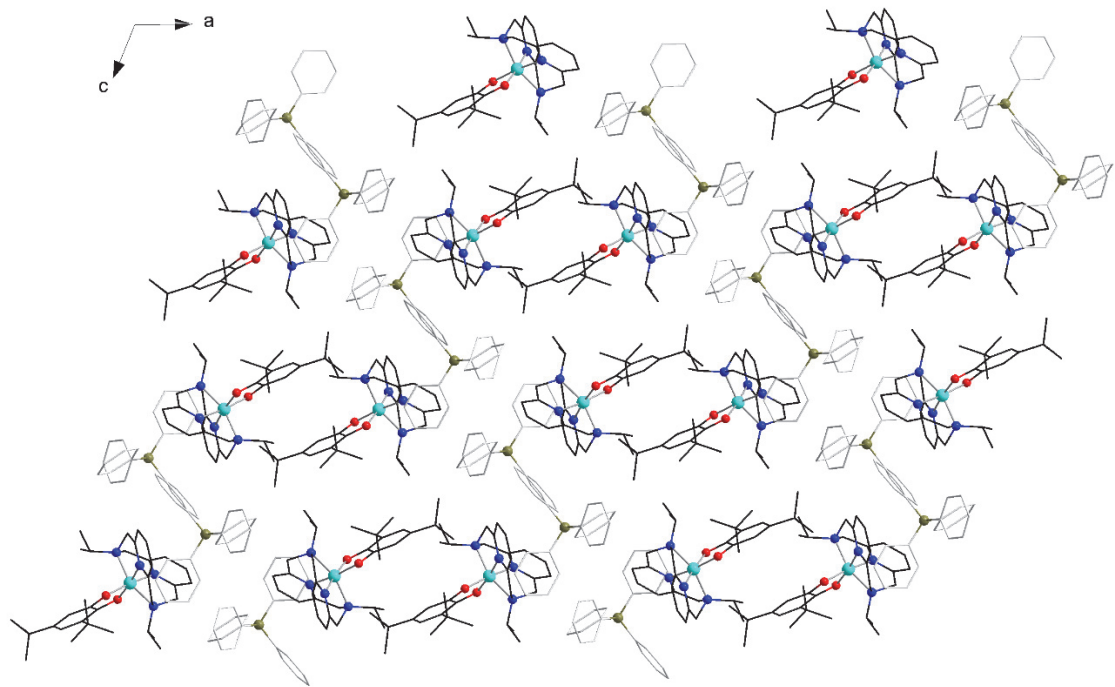


Fig. S1 Crystal packing diagrams for **1a**·dioxane and **4a**·2MeOH.

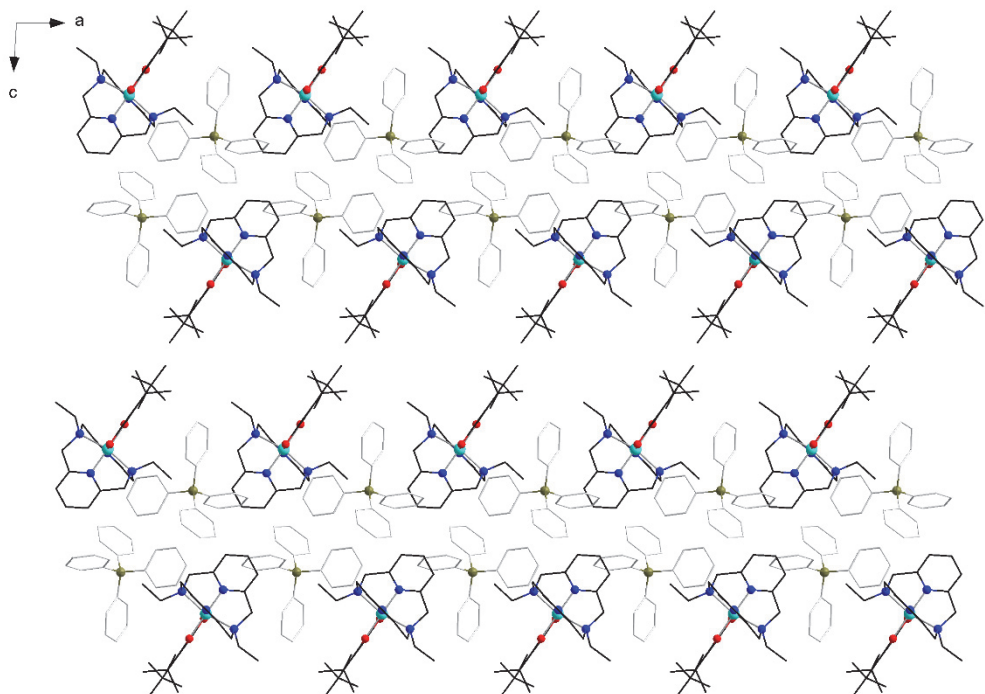


Fig. S2 Crystal packing diagrams for compounds **2a**·2dioxane and **3a**·1.5dioxane.

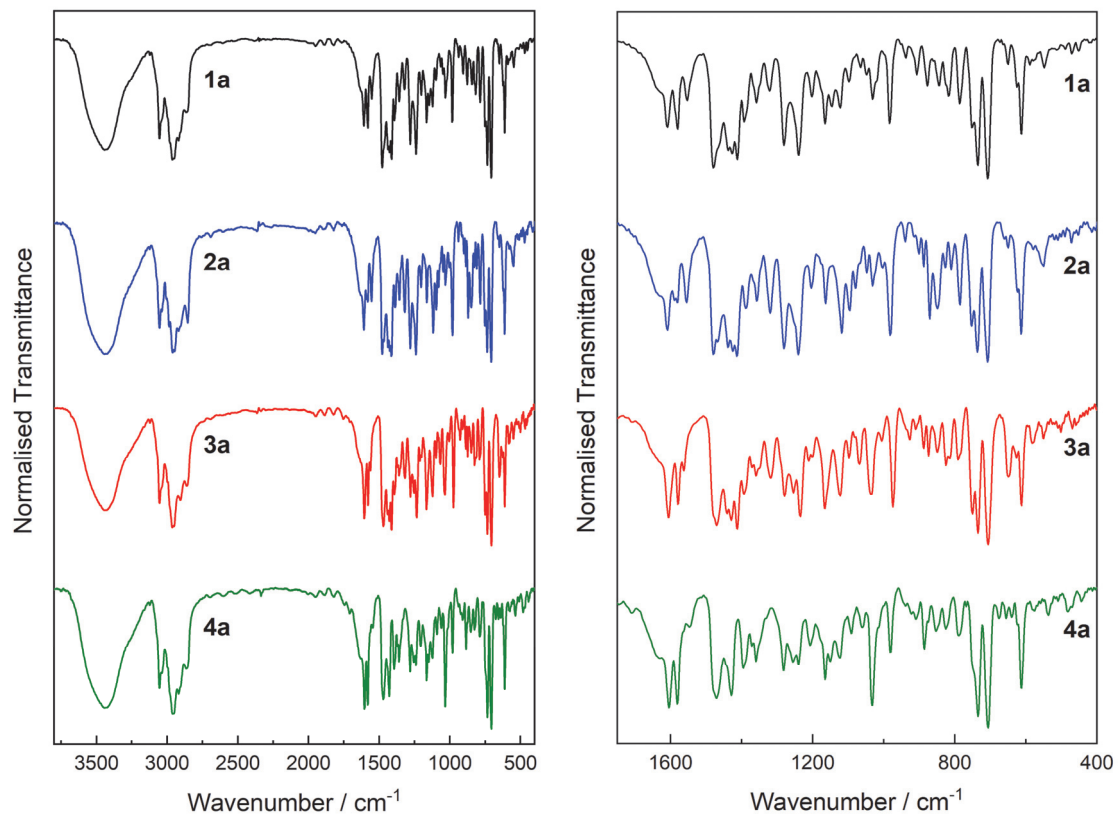


Fig. S3 Infrared spectra (pressed KBr disks) for, from top to bottom: **1a**·dioxane, **2a**·2dioxane, **3a**·1.5dioxane and **4a**·dioxane; complete spectra (left) and fingerprint region (right).

Table S2 Electronic (UV-visible) absorption spectral bands for solutions of compounds **1a**, **2a**, **3a** and **4a** at 293 K in acetonitrile (MeCN), butyronitrile (BuCN) and 1,2-dichloroethane (DCE).

Compound	Absorption maxima, λ_{max} / nm (ϵ / M ⁻¹ cm ⁻¹)			Assignment ^a	References
	Solvent				
	MeCN	BuCN	DCE		
1a	307 (14,709)	307 (12,733)	307 (10,844)	CT (L-N ₄ R ₂)	ref. 2
	420 (978)	408 (1,281)	405 (3,633)	d-d (Co(III))	ref. 3
			585 (536)	d-d Co(II) or MLCT	ref. 3–5
			664 (668)	MLCT	ref. 3,5
2a	307 (16,854)	308 (18,384)	310 (14,441)	CT (L-N ₄ R ₂)	ref. 2
	~400	~400	412 (1112)	d-d (Co(III))	ref. 3
			646 (150)	MLCT	ref. 3,5
3a	288 (12,060) sh	288 (9,615) sh	287 (6506) sh	CT (L-N ₄ R ₂)	ref. 2
	~400	~400	398 (1866)	d-d (Mn(III))	ref. 6
4a	~280	~280	~280	CT (L-N ₄ R ₂)	ref. 2
	~390	-390	~390	d-d (Fe(III))	ref. 7
	580 (2,832)	594 (2,226)	627 (2,607)	LMCT	ref. 8,9
	770 (2,997)	803 (2,340)	862 (2,660)	LMCT	ref. 8,9

^a CT = charge transfer, LMCT = ligand to metal charge transfer, MLCT = metal to ligand charge transfer

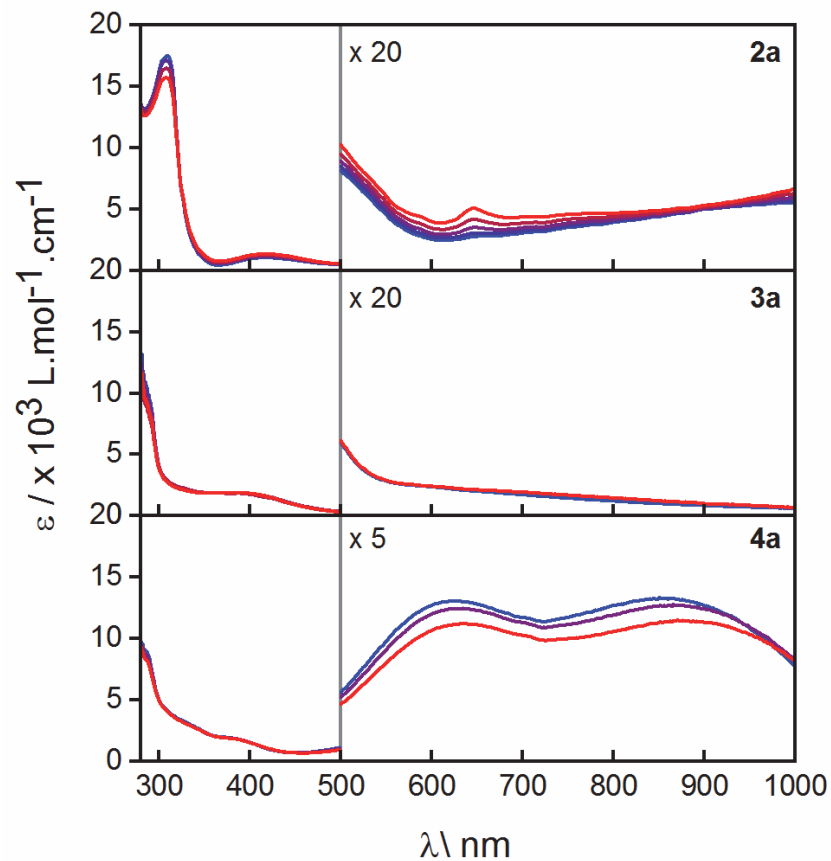


Fig. S4 Variable temperature absorption spectra of **2a** in 1,2-dichloroethane, **3a** in butyronitrile and **4a** in 1,2-dichloroethane (from top to bottom) from 293 K to 333 K.

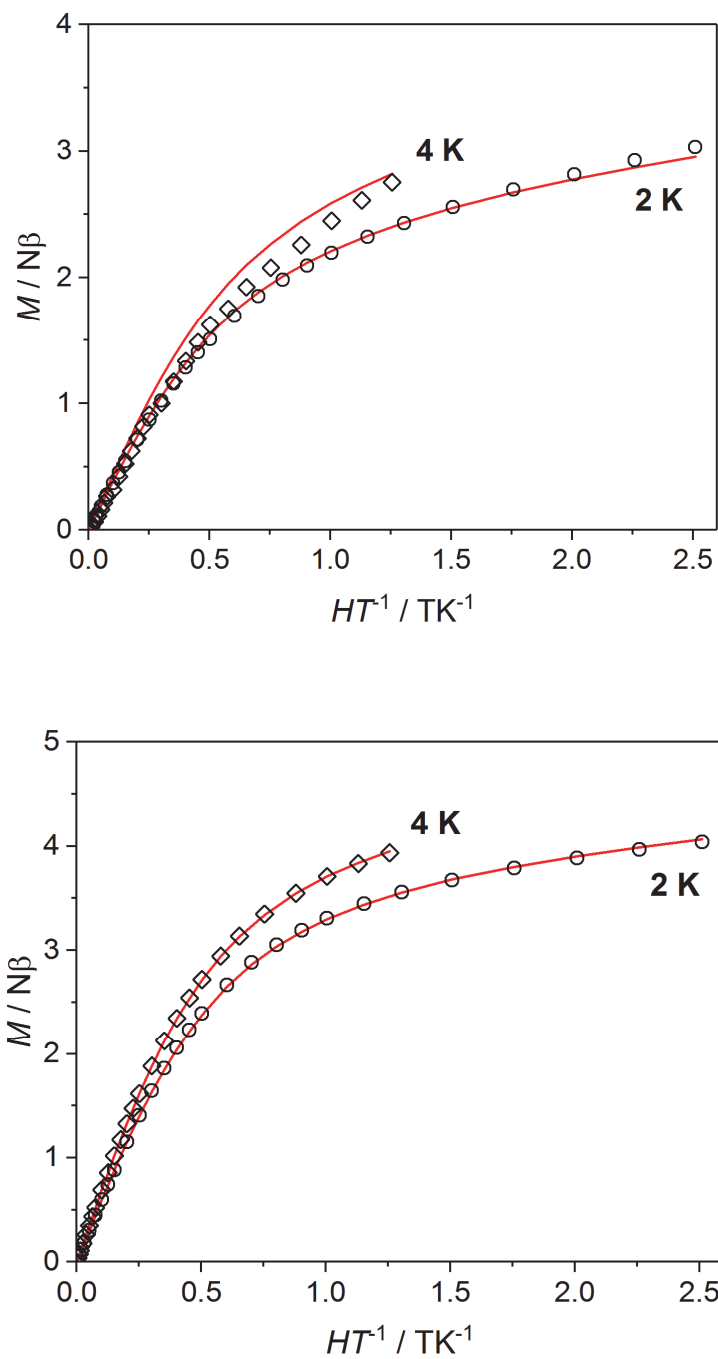


Fig. S5 Plots of reduced magnetization measured for **3a**·1.5dioxane (top) and **4a**·dioxane (bottom) in the solid state at 2 and 4 K; the lines are best fits as described in the text.

Table S3 Experimental and calculated Mössbauer parameters of **4a**-dioxane. Parameters calculated using B3LYP Def2-TZVP; Fe CP(PPP) + COSMO(Water) and using the calibration of Roemelt et al.¹⁰

Method	Species	δ (mm/s)	ΔE_Q (mm/s)
experimental	4a	0.43	2.08
calculated	LS-Fe(III)-dbcat	0.23	2.49
	IS-Fe(III)-dbcat	0.28	2.28
	HS-Fe(III)-dbcat	0.53	2.08

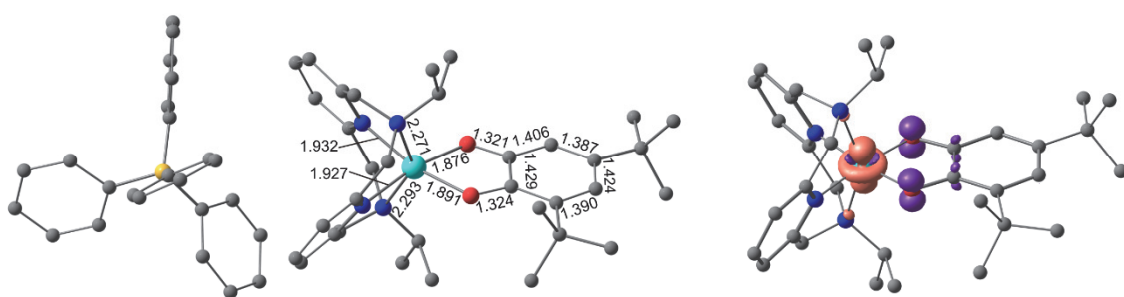
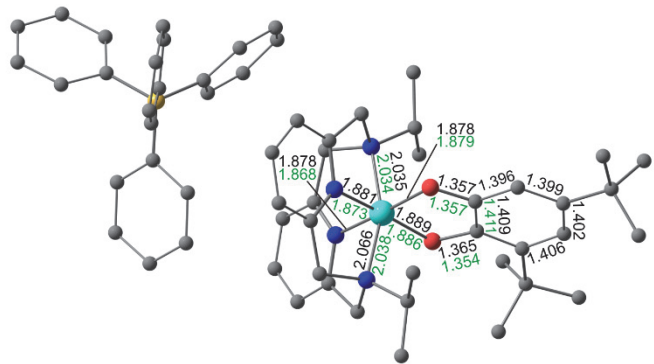
Table S4 Calculated spin states taking into account exchange interactions (S), relative energies (ΔE) and exchange spin coupling constants (J) of the electromers of compounds **1a**, **2a**, **5b**, **6a**, **3a**, **4a** calculated by the DFT UTPSSh/6-311++G(d,p) method.

Compound	Ancillary ligand	Electromer	S	ΔE (kcal mol $^{-1}$) ¹⁾	J (cm $^{-1}$)	Reference
1a	L-N ₄ iPr ₂	LS-Co(III)-dbcat	0	0.0	-	this work
		LS-Co(II)-dbsq	1	-0.2	861	
		HS-Co(II)-dbsq	2	4.6	-18	
2a	L-N ₄ Et ₂	LS-Co(III)-dbcat	0	0.0	-	this work
		LS-Co(II)-dbsq	1	2.6	741	
		HS-Co(II)-dbsq	2	10.9	-7	
5b	L-N ₄ Me ₂	LS-Co(III)-dbcat	0	0.0	-	ref. 11
		LS-Co(II)-dbsq	1	5.5	769	
		HS-Co(II)-dbsq	2	12.5	-38	
6a	L-N ₄ tBu ₂	LS-Co(II)-dbsq	1	0.0	727	ref. 11
		LS-Co(III)-dbcat	0	4.7	-	
		HS-Co(II)-dbsq	2	6.9	-29	
3a	L-N ₄ iPr ₂	HS-Mn(III)-dbcat	2	0.0	-	this work
		HS-Mn(II)-dbsq	2	6.1	-225	
		IS-Mn(III)-dbcat	1	8.8	-	
4a	L-N ₄ iPr ₂	LS-Fe(III)-dbcat	1/2	0.0	-	this work
		IS-Fe(III)-dbcat	3/2	4.7	-	
		HS-Fe(III)-dbcat	5/2	7.9	-	

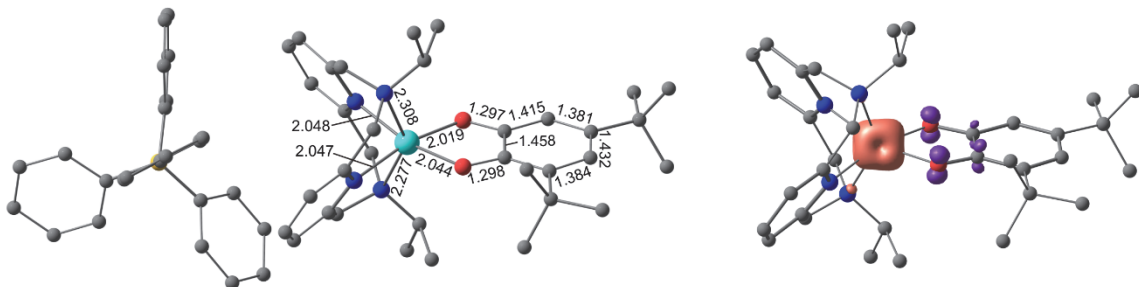
Table S5 Spin states (S), total energies without (E) and with (E^{ZPE}) taking into account for zero-point harmonic vibrations, expectation values of the spin-squared operator (\hat{S}^2) and amount of spin density at metal center (q_s^M) of the electromers of the compounds **1a**, **2a**, **3a**, **4a**, **5b** and **6a** calculated by DFT UTPSSh/6-311++G(d,p) method.

Compound	Electromer	S	E (a.u.)	E^{ZPE} (a.u.)	\hat{S}^2	q_s^M
1a	LS-Co(III)-dbcatt	0	-4029.141511	-4028.009107	0.000	0.00
	LS-Co(II)-dbsq	1	-4029.141896	-4028.012497	2.016	1.15
	LS-Co(II)-dbsq BS	0	-4029.137872	—	0.990	
	HS-Co(II)-dbsq	2	-4029.134182	-4028.006246	6.011	2.60
	HS-Co(II)-dbsq BS	1	-4029.134442	—	2.898	
2a	LS-Co(III)-dbcatt	0	-3950.493781	-3949.417978	0.000	0.00
	LS-Co(II)-dbsq	1	-3950.489633	-3949.416240	2.016	1.17
	LS-Co(II)-dbsq BS	0	-3950.486185	—	0.994	
	HS-Co(II)-dbsq	2	-3950.476361	-3949.404898	6.012	2.66
	HS-Co(II)-dbsq BS	1	-3950.476459	—	2.898	
5b^a	LS-Co(III)-dbcatt	0	-3030.073713	-3029.626623	0.000	0.00
	LS-Co(II)-dbsq	1	-3030.064881	-3029.620263	2.017	1.20
	LS-Co(II)-dbsq BS	0	-3030.060000	—	0.623	
	HS-Co(II)-dbsq	2	-3030.053738	-3029.610513	6.011	2.70
	HS-Co(II)-dbsq BS	1	-3030.054283	—	2.890	
6a^a	LS-Co(III)-dbcatt	0	-5631.676780	-5630.751672	0.000	0.00
	LS-Co(II)-dbsq	1	-5631.684261	-5630.760971	2.016	1.14
	LS-Co(II)-dbsq BS	0	-5631.680736	—	0.952	
	HS-Co(II)-dbsq	2	-5631.673230	-5630.751861	6.012	2.64
	HS-Co(II)-dbsq BS	1	-5631.672831	—	2.909	
3a	IS-Mn(III)-dbcatt	1	-3797.400005	-3796.269587	2.037	1.88
	HS-Mn(III)-dbcatt	2	-3797.414000	-3796.285316	6.035	3.80
	HS-Mn(II)-dbsq	3	-3797.398984	-3796.271935	12.013	4.72
	HS-Mn(II)-dbsq BS	2	-3797.404219	—	6.910	
4a	LS-Fe(III)-dbcatt	1/2	-3910.108809	-3908.977745	0.791	0.57
	IS-Fe(III)-dbcatt	3/2	-3910.101254	-3908.971851	3.784	2.53
	HS-Fe(III)-dbcatt	5/2	-3910.096182	-3908.967716	8.762	3.82

^a From ref. 11



LS-Co(II)-dbsq



HS-Co(II)-dbsq

Fig. S7 Optimized geometries and spin density distribution in the isomeric forms of compound **1a** calculated by DFT UTPSSh/6-311++G(d,p) method (cutoff = 0.02). Hereinafter hydrogen atoms are omitted; bond lengths are given in Å, X-ray data are indicated in green.

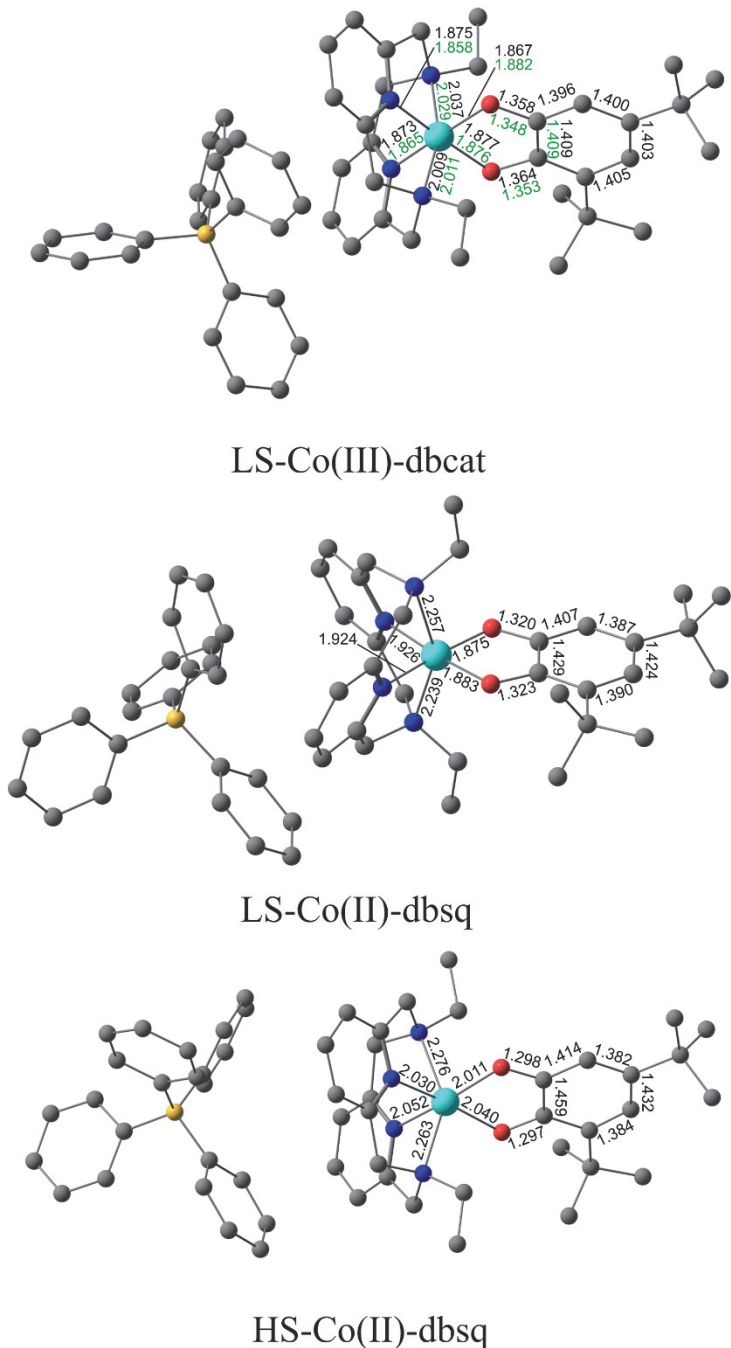
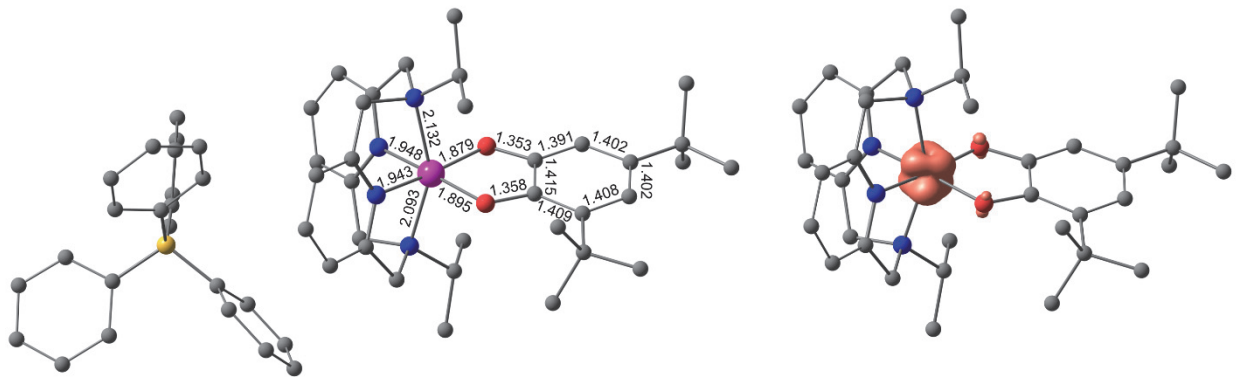
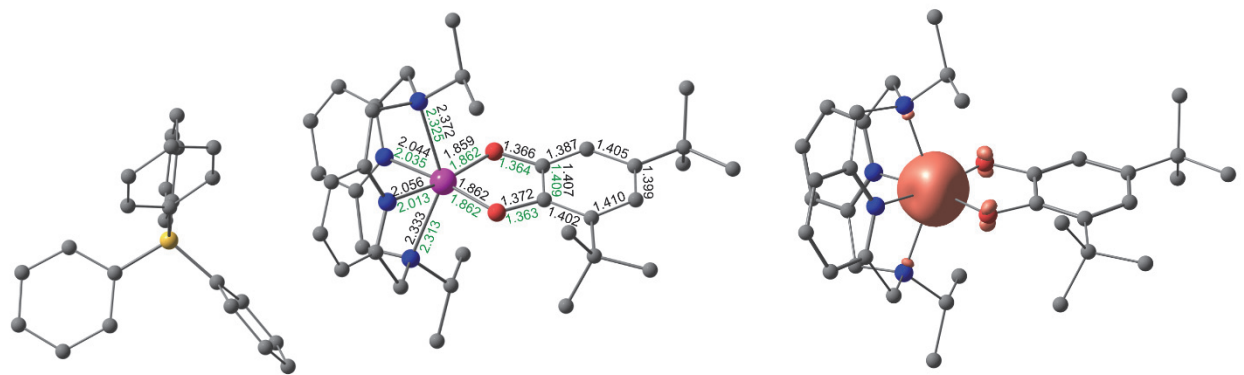


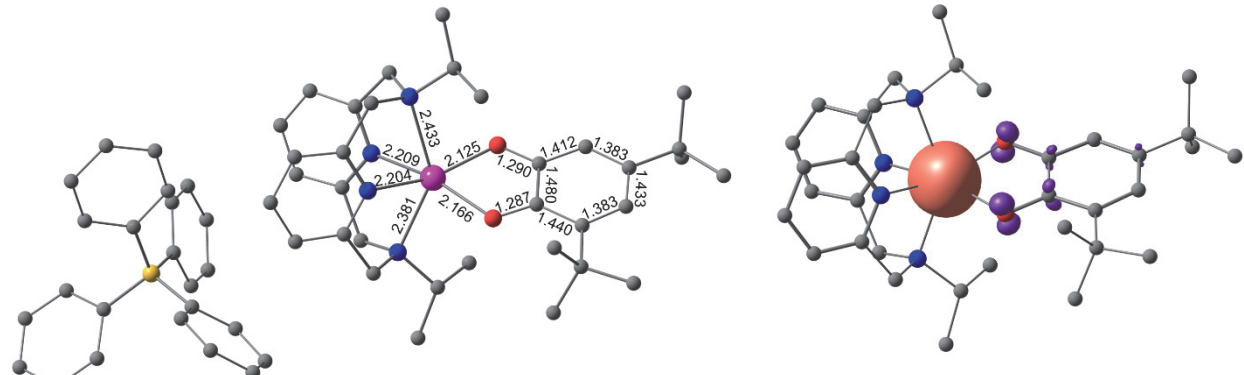
Fig. S8 Optimized geometries of the isomeric forms of compound **2a** calculated by DFT UTPSSh/6-311++G(d,p) method (cutoff = 0.02).



IS-Mn(III)-dbcatalyst



HS-Mn(III)-dbcatalyst



HS-Mn(II)-dbsq

Fig. S9 Optimized geometries and spin density distribution in the isomeric forms of compound **3a** calculated by DFT UTPSSh/6-311++G(d,p) method (cutoff = 0.02).

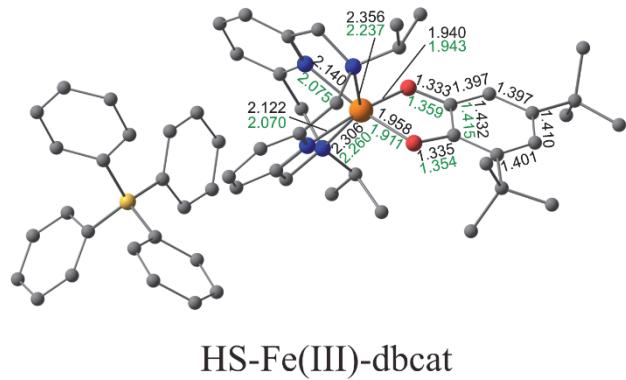
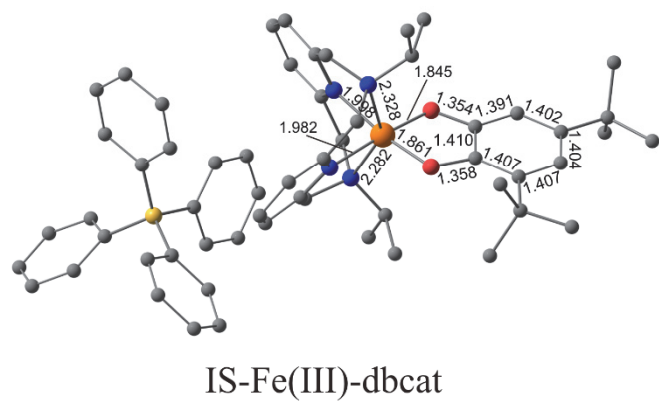
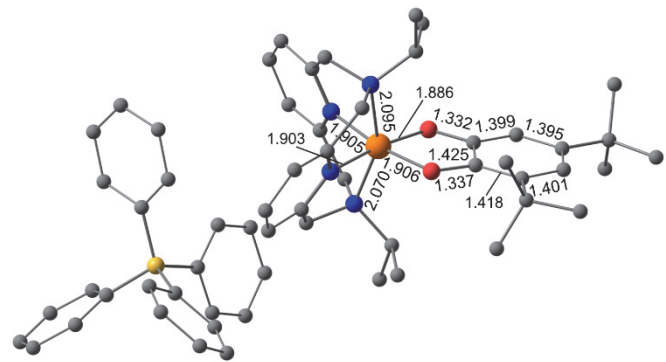


Fig. S10 Optimized geometries of the isomeric forms of the compound **4a** calculated by DFT UTPSSh/6-311++G(d,p) method.

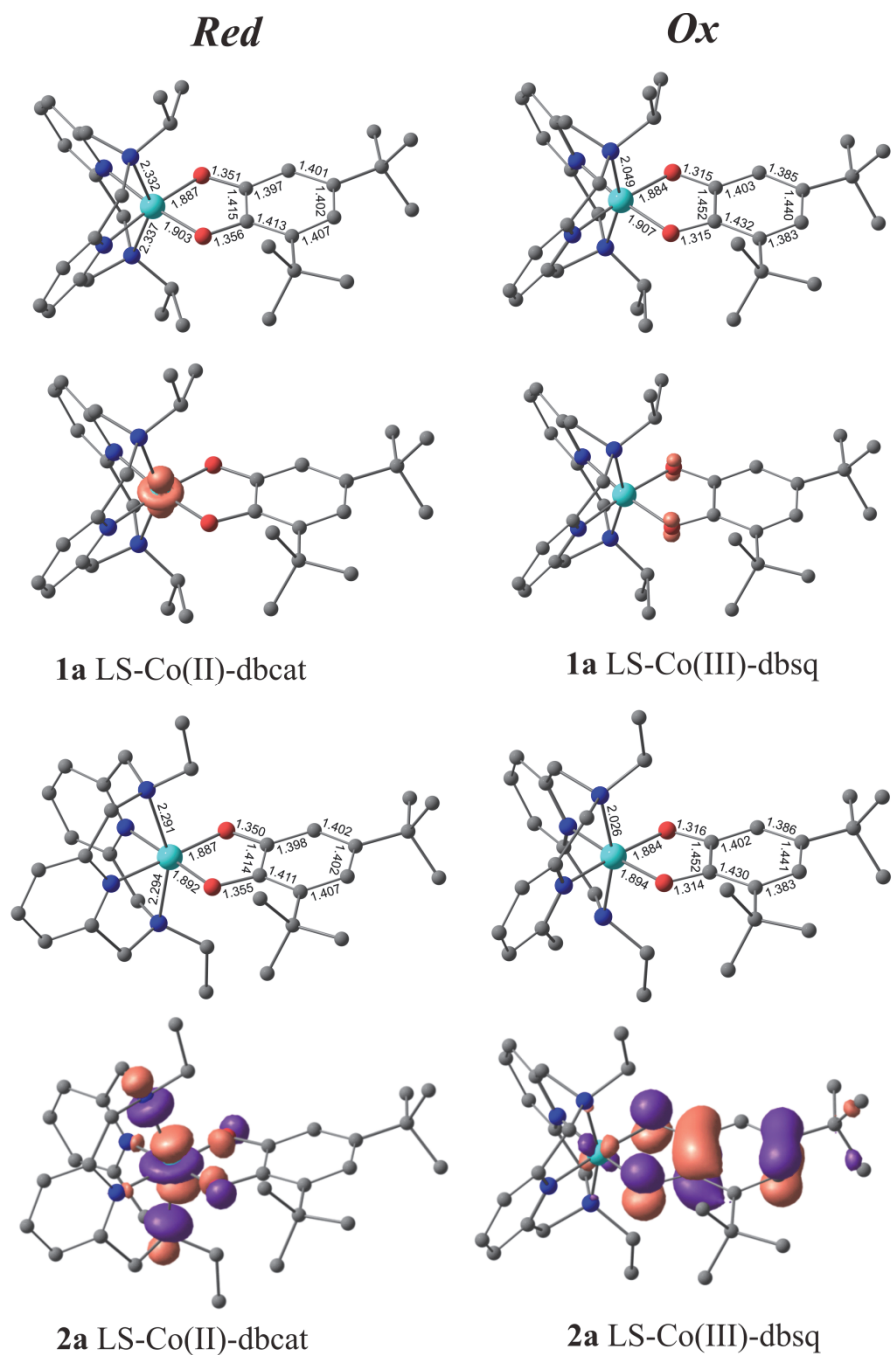


Fig. S11 Optimized geometries of the *red* (left) and *ox* (right) forms of complexes **1** in **1a** and **2** in **2a**, spin density distribution in the *red* (left) and *ox* (right) forms of **1** and the shapes of SOMOs of the *red* (left) and *ox* (right) forms of **2** calculated by DFT UTPSSh/6-311++G(d,p) method.

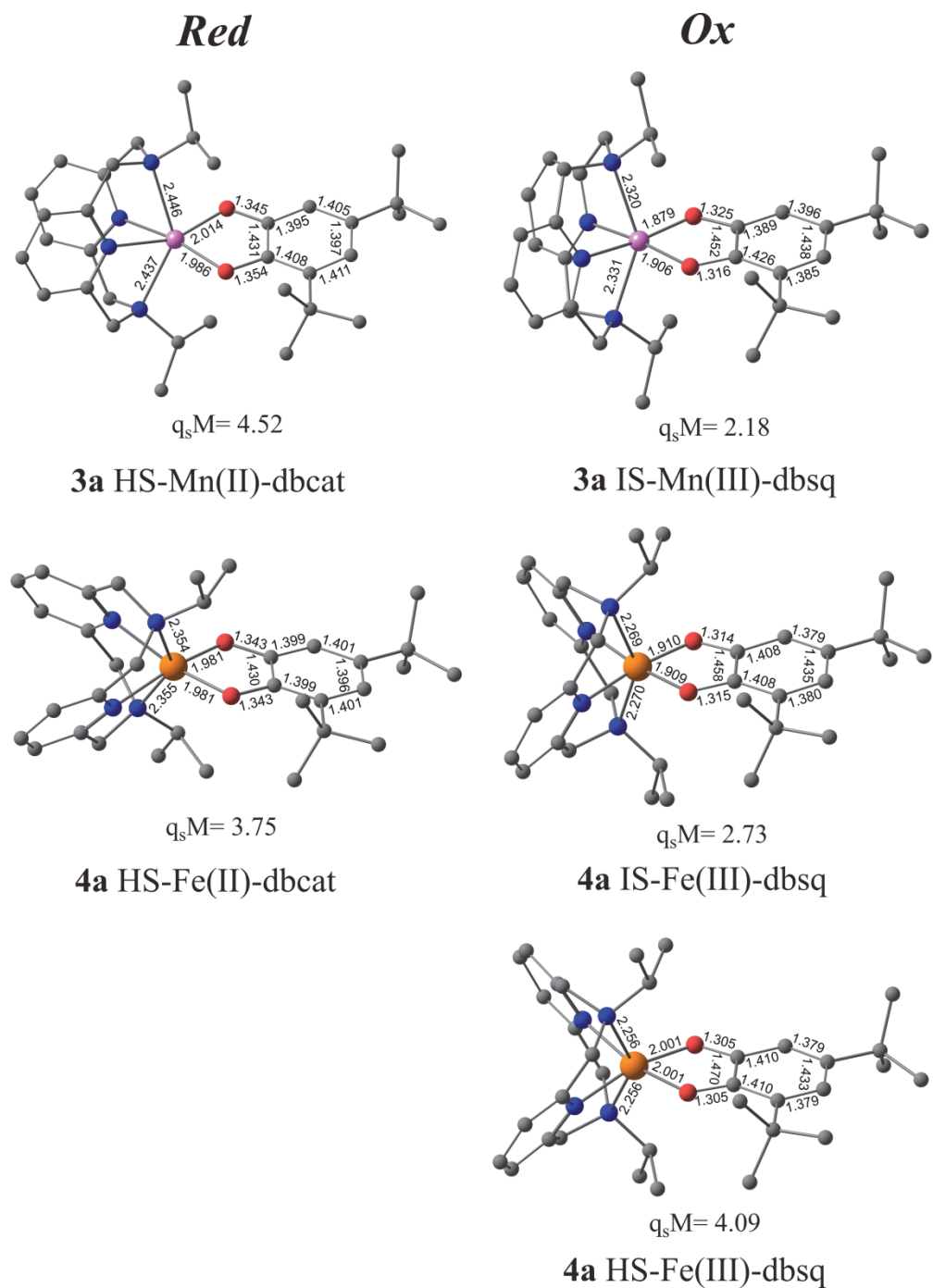


Fig. S12 Optimized geometries and spin densities ($q_s M$) at the metal centers of the *red* (left) and *ox* (right) forms of complexes **3** in **3a** and **4** in **4a** calculated by DFT UTPSSh/6-311++G(d,p) method.

Table S6 Charge (q), spin (S), total energy (E_{total}), total energy with taking into account for non-specific solvation ($E_{\text{total}}^{\text{solv}}$) (SMD, solvent – acetonitrile) and thermal correction to Gibbs Free Energy (all values are given in a.u.) of the various redox forms of complexes **1** in **1a** and **2** in **2a** calculated by DFT UTPSSh/6-311++G(d,p) method.^a

State	Electromer	q	S	E_{total}	$E_{\text{total}}^{\text{solv}}$	Gibbs Correction
1a red	LS-Co(II)-dbc _{cat}	0	1/2	-3077.381663	-3077.428893	0.690716
1a	LS-Co(III)-dbc _{cat}	+1	0	-3077.209743	-3077.310517	0.698295
1a ox	LS-Co(III)-db _{sq}	+2	1/2	-3076.924203	-3077.158139	0.699879
2a red	LS-Co(II)-dbc _{cat}	0	1/2	-2998.729200	-2998.779807	0.636402
2a	LS-Co(III)-dbc _{cat}	+1	0	-2998.561783	-2998.665944	0.644620
2a ox	LS-Co(III)-db _{sq}	+2	1/2	-2998.275207	-2998.513034	0.645701

^a Computational details necessary for the redox potential calculations in accordance with refs 12 and 13

References

- 1 S. Alvarez, D. Avnir, M. Llunell and M. Pinsky, *New J. Chem.*, 2002, **26**, 996–1009.
- 2 J. R. Khusnutdinova, J. Luo, N. P. Rath and L. M. Mirica, *Inorg. Chem.*, 2013, **52**, 3920–3932.
- 3 A. Beni, A. Dei, S. Laschi, M. Rizzitano and L. Sorace, *Chem. Eur. J.*, 2008, **14**, 1804–13.
- 4 H. J. Krüger, *Chem. Ber.*, 1995, **128**, 531–539.
- 5 A. Caneschi, A. Dei, D. Gatteschi and V. Tangoulis, *Inorg. Chem.*, 2002, **41**, 3508–3512.
- 6 B. Albela, R. Carina, C. Policar, S. Poussereau, J. Cano, J. Guilhem, L. Tchertanov, G. Blondin, M. Delroisse and J. J. Girerd, *Inorg. Chem.*, 2005, **44**, 6959–6966.
- 7 W. O. Koch, V. Schünemann, M. Gerdan, A. X. Trautwein and H.-J. Krüger, *Chem. Eur. J.*, 1998, **4**, 1254–1265.
- 8 W. O. Koch and H.-J. Krüger, *Angew. Chemie Int. Ed. English*, 1995, **34**, 2671–2674.
- 9 P. Mialane, L. Tchertanov, F. Banse, J. Sainton and J. J. Girerd, *Inorg. Chem.*, 2000, **39**, 2440–2444.
- 10 M. Römelt, S. Ye and F. Neese, *Inorg. Chem.*, 2009, **48**, 784–785.
- 11 A. A. Starikova, M. G. Chegrev, A. G. Starikov and V. I. Minkin, *Comput. Theor. Chem.*, 2018, **1124**, 15–22.
- 12 A. V. Marenich, J. Ho, M. L. Coote, C. J. Cramer and D. G. Truhlar, *Phys. Chem. Chem. Phys.*, 2014, **16**, 15068–15106.
- 13 L. E. Roy, E. Jakubikova, M. Graham Guthrie and E. R. Batista, *J. Phys. Chem. A*, 2009, **113**, 6745–6750.